

# Continuous Separation of Lignin from Organosolv Pulping Liquors: Combined Lignin Particle Formation and Solvent Recovery

Peter Schulze,<sup>\*,†</sup> Moritz Leschinsky,<sup>‡</sup> Andreas Seidel-Morgenstern,<sup>†</sup> and Heike Lorenz<sup>†</sup>

<sup>†</sup>Max Planck Institute for Dynamics of Complex Technical Systems (MPI DCTS), 39106 Magdeburg, Germany

<sup>‡</sup>Fraunhofer Center for Chemical-Biotechnological Processes (CBP), 06237 Leuna, Germany

## Supporting Information

**ABSTRACT:** The solubility and softening behavior of lignin from acid-catalyzed ethanol/water pulping was determined in various ethanol/water solvent mixtures and a process relevant temperature range. Operation conditions for an optimized lignin separation process have been derived from the determined lignin phase behavior. A continuous lignin separation and solvent recovery process has been developed in lab scale and was successfully up-scaled to a dedicated pilot plant at Fraunhofer CBP (WO2016062676A1). Agglomeration of softened lignin particles and lignin “stickiness” were adjusted by temperature (38–44 °C at 80–120 mbar) and ethanol content of the lignin dispersion (6–9 wt %). In this manner, ethanol recovery by evaporation and lignin particle formation were facilitated simultaneously, which was monitored by inline infrared spectroscopy. The agglomeration behavior of different lignins was monitored via inline particle size analysis. Optimal process conditions resulted in good filterability of the lignin dispersion with average filter cake resistances of  $10^{11}$  to  $10^{13}$  m<sup>-2</sup> and lignin yields close to 100 wt % of water-insoluble lignin.



## 1. INTRODUCTION

Lignocellulose biorefineries are supposed to provide renewable chemicals, like sugars from cellulose and hemicellulose and phenolics from lignin, from woody biomass to the chemical industry in the midterm future. The chemical industry has to become more defossilized and sustainable, making the utilization of renewable carbon-sources necessary.<sup>1,2</sup>

About 5% of the lignin currently processed in the worldwide pulping industry is separated as a product with different application areas.<sup>3</sup> Various processes (e.g., LignoBoost,<sup>4–6</sup> LignoForce<sup>7</sup>) for the separation of lignin from alkaline black liquors (from e.g. Kraft, Sulfite, Soda pulping) have been developed and realized in commercial pulping plants.<sup>8,9</sup> However, the quality of the obtained lignins is inferior compared to lignins produced by an organosolv (organic solvent) pulping process in terms of, e.g. odor, sulfur and ash content.<sup>10</sup>

Efficient separation processes are essential for the economic viability of lignocellulose biorefineries that apply organosolv pulping to fractionate woody biomass. The organic solvent recycling and the accompanying lignin separation processes have a great impact on the energy consumption of the refinery.<sup>11,12</sup> Processes for the separation of lignin from organosolv pulping liquors have already been developed in the past.<sup>13–17</sup> Besides the development of membrane separation techniques<sup>18,19</sup> and a liquid–liquid extraction process,<sup>20</sup> two general methods for lignin precipitation are usually described in the literature: (a) dilution of pulping liquor with water or another aqueous process stream and (b)

direct evaporation of ethanol from the pulping liquor. The first and most commonly used method (a) can lead to lignin dispersions with poor filtration properties due to small particle sizes and to a multiple increase in process streams of filtrate.<sup>15–17,21–25</sup> The second method (b) can lead to lignin incrustations in the apparatus due to the precipitation of a soft and sticky lignin phase. These disadvantages of the state-of-the-art lignin separation processes result in increased operation and investment costs, lowering economic viability of the whole biorefinery.<sup>13,14,23,26</sup>

The complete recovery of ethanol can be hindered by the formation of ethyl glycosides that bind ethanol to carbohydrate constituents of the lignocellulose.<sup>27</sup> However, it was recently implicated that those ethyl glycosides tend to decompose during ethanol recovery by distillation.<sup>28</sup> Even though it is important to close the ethanol cycle as complete as possible in order to minimize the input of makeup solvent, the focus of this work was on lignin recovery and particle formation.

Thus in this work, an improved lignin separation process on the basis of a fundamental understanding of the lignin phase behavior was developed in cooperation with the Fraunhofer Center for Chemical-Biotechnological Processes (CBP). The CBP operates a lignocellulose biorefinery pilot plant with a 400 L batch forced-circulation reactor for organosolv pulping of

**Received:** September 29, 2018

**Revised:** February 11, 2019

**Accepted:** February 12, 2019

**Published:** February 12, 2019

**Table 1.** Overview of the Batch-Wise Applied Pulping Conditions, Measured Pulping Liquor Compositions and Molar Weights of the Investigated Lignins<sup>a</sup>

Pulping batch No.	Lignocellulose type	Pulping temp. (°C)	Sulfuric acid (wt % of dry wood)	Ethanol in pulping solvent (wt %)	Time at pulping temperature (minutes)	Lignin in pulping liquor (wt %)	Ethanol in pulping liquor (wt %)	Number avg. molecular mass of lignin ( $M_n$ ) (g/mol)	Weight avg. molecular mass of lignin ( $M_w$ ) (g/mol)	Polydispersity $M_w/M_n$ (-)
K1	beech	170	0.5	50	90	2.2	47.2	1056	3949	3.738
K6	beech	170	0.5	50	90	n.a.	n.a.	1197	4069	3.4
K8	beech	170	0.5	50	90	n.a.	n.a.	842.3	2737	3.249
K9	beech	170	0.5	50	90	2.6	44.2	1108	4903	4.426
K29	beech	170	0.5	50	90	2	50.7	1017	5327	5.236
K37	beech	190	0.5	50	180	1.86	45.23	1101	3041	2.762
K39	beech	180	1	50	180	2.41	43.81	961.9	2212	2.3
K40	beech	170	1	50	180	2.04	45.42	977.6	2494	2.551
K41	beech	190	1	50	180	2.53	44.9	884.3	1949	2.204
K42	beech	180	0	50	180	1.93	44.17	1085	3298	3.04
K43	beech	170	0.5	50	180	1.72	45.18	1183	3778	3.194
K44	beech	190	0	50	180	2.21	45.33	944.9	2329	2.465
K45	beech	170	0	50	200	1.49	44.02	1162	5868	5.052
F02	spruce	170	1.1	65	90	2.8	55	823	2146	2.608
K103	beech	170	1	50	90	2.3	46.39	1045	2816	2.693
K128	eucalyptus	170	1	50	90	3.35	43.35	1046	3014	2.882
K138	beech	170	0.8	50	145	1.35	47.2	819.2	2160	2.636
K139	beech	170	0.8	50	145	1.35	n.a.	n.a.	n.a.	n.a.

<sup>a</sup>n.a.: not analyzed.

wood chips and other woody biomass. The patented process was up-scaled to the pilot plant facilities at Fraunhofer CBP<sup>29</sup> and facilitates simultaneous precipitation and controlled agglomeration of lignin from organosolv pulping liquors on the basis of phase behavior and softening properties of lignin. Improved filterability of the produced lignin dispersion, prevention of lignin incrustations, full lignin recovery and decreased down-streams (aqueous hemicellulose solution after lignin filtration) are the main achievements of the process.

In the following, at first the determination of lignin particle softening and agglomeration behavior is described. From this knowledge, process conditions suitable for the lignin particle formation are derived and put into operation, first in a continuous lab-scale separation process. The extension of the lab-plant by installing a falling film evaporator to prevent foaming during solvent evaporation is then described. Finally, results of the first successful trials in the reconstructed pilot plant are presented.

## 2. MATERIALS AND METHODS

**2.1. Materials.** The investigated pulping liquors and lignins from these pulping liquors were produced in the lignocellulose biorefinery pilot plant at Fraunhofer CBP in Leuna as already described in a previous journal article.<sup>30</sup> Table 1 gives an overview of the lignocellulosic raw materials and the pulping conditions at which the investigated pulping liquors were produced. Beech, spruce and eucalyptus wood chips (70 kg dry wood mass per 400 L batch) have been typically pulped at temperatures between 170 and 190 °C, in 50 (or 65) wt % aqueous ethanol solvent with sulfuric acid contents between 0 and 1.1 wt % (referred to dry wood mass) for 90 min (up to 180 min for study of reaction kinetics).

**2.2. Methods and Procedures.** **2.2.1. Analytical Methods.** The main analytical methods used are described in the following. More detailed information can be found in the author's dissertation.<sup>31</sup>

**2.2.1.1. Pulping Liquors and Process Solutions. Gravimetric Analysis.** The lignin and sugar mass fraction in pulping liquor was determined gravimetrically. The solution was dried and the masses of the initial solution and of the dry substance were determined. Drying was carried out usually in a vacuum oven at around 60 °C and down to 10 mbar until the pressure remained constant after turning off the pump, meaning that no further liquid evaporated into the gas phase. The dry solids of the pulping liquor were assumed to be a mixture of water-solubles (named "sugars") and water insolubles (named "lignin"). The dry solids were suspended in water in order to dissolve the water-soluble sugar fraction. The water insoluble solid lignin fraction was dried after filtration as described above. Then the mass fractions of lignin and sugars in the pulping liquors were calculated. The content of dissolved (and dispersed) dry substances in process streams of the pilot plant was determined by an Infrared Moisture Analyzer (Sartorius).

**Headspace Gas Chromatography (GC-hs).** GC-hs has been utilized to measure the ethanol mass fraction in aqueous mixtures containing also lignin, sugars and other pulping liquor constituents. Samples were prepared with 1 wt % of acetonitrile as internal standard and were diluted with deionized water to ethanol contents below 10 wt % to measure inside the calibration range. Samples were equilibrated in the headspace device (Agilent 7697A) for 20 min at 85 °C and shaking. After injection the column (Agilent J&W VF-624 ms, 30 m, 0.25 mm, 1.4 μm) was heated from 40 to 150 °C at 10 K/min in the GC device (Agilent 6890N) and the components were detected by a flame ionization.

**2.2.1.2. Lignin Characterization. High Performance Size Exclusion Chromatography (HPSEC).** HPSEC was performed at the Fraunhofer CBP in Leuna for molecular mass determination. Lignin samples were dissolved in the eluent at a concentration of about 0.4 wt %, filtered through a 0.1 μm filter and 100 μL were injected to the chromatographic analysis. AppliChrom ABOA DMSO-Phil-P350 and DMSO-

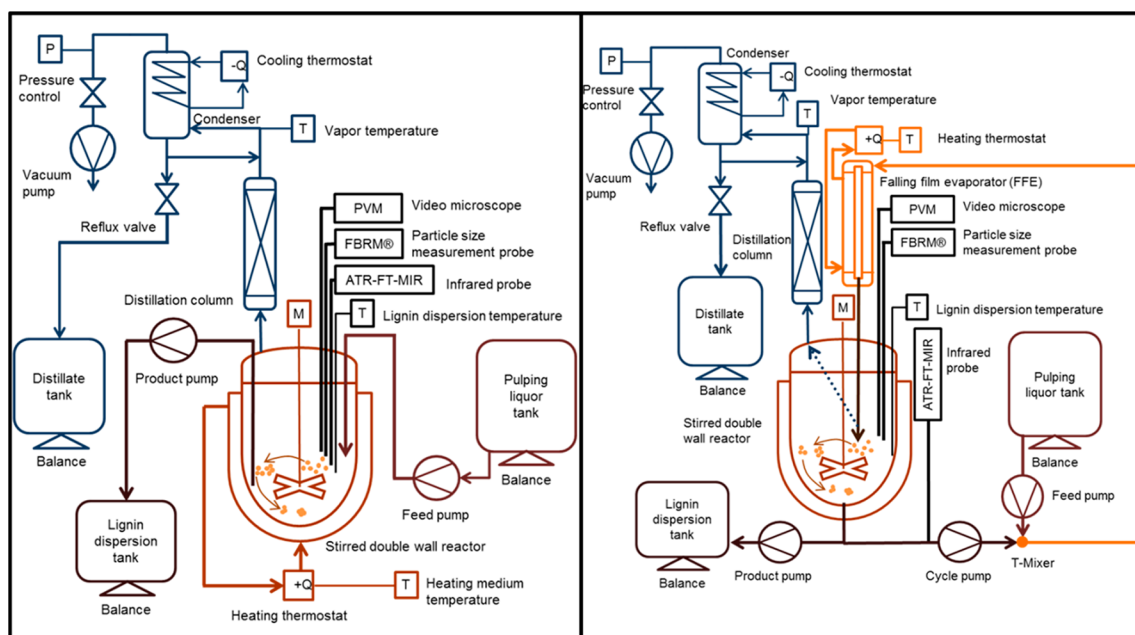


**Figure 1.** Flowsheet of the lab plant for continuous lignin precipitation without (left) and with (right) falling film evaporator.

Phil-P-250 columns were used at 80 °C with DMSO + 0.075 mol/L sodium nitrate as eluent at 0.5 mL/min flow to resolve the lignin molecules by size. A refractive index detector was applied to measure the elution profile at 40 °C and the software “Parsec” for interpretation. The method was calibrated with dextran standards with  $M_w$  between 180 and 11260 g/mol.

**2.2.1.3. Inline Process Analytics. Infrared Spectroscopy.** Attenuated total reflection Fourier transform mid-infrared (ATR-FT-MIR) spectroscopy (ReactIR45m, Mettler Toledo) has been used to measure spectra of the lignin dispersion inline. The silver halide optical fiber and the diamond optical window allow to collect spectra in the wavenumber range of 1900 to 650  $\text{cm}^{-1}$ . A univariate calibration model has been used to determine the ethanol concentration in the aqueous phase of the lignin dispersion during lignin precipitation processes. The univariate model was calibrated in-process by measuring spectra and taking samples of the dispersion. The ethanol content of the samples was determined by GC-hs. The measured ethanol contents have been linearly fitted to the peak height at wavenumber 1046  $\text{cm}^{-1}$  (relative to the basepoint at 1067  $\text{cm}^{-1}$ ) of the MIR spectra.

**Focused Beam Reflectance Measurement.** The Particle Track G400 probe with focused beam reflectance measurement technology (FBRM) from Mettler Toledo was utilized to monitor the changes of the chord length distribution of lignin particles, agglomerates and droplets during several experiments. The technology is based on the backscattering of a rotating laser beam from particles flowing in front of the probe window. As particles can be scanned at smaller or larger parts than their average size, the detected value is called “chord length” instead of “particle size”. In this work the term “size” is used instead of “chord length” since the shape of the measured particles is close to spherical.

**Video Microscopy.** The V19 video microscope with PVM (Particle Vision and Measurement) technique from Mettler Toledo was applied additionally to the FBRM probe in order to elucidate the mechanisms between the particles causing changes of the particle chord length distribution (e.g.,

agglomeration and coalescence). The probe provided pictures with about 2  $\mu\text{m}$  optical resolution. Aggregates of primary lignin particles and the formation of aggregates could be imaged.

**2.2.2. Experimental Procedures. 2.2.2.1. Determination of Softening and Agglomeration Temperatures of Lignin in Aqueous Dispersions.** A method for the measurement of agglomeration (softening) temperatures of lignin particles was conducted by utilization of the “Crystalline” reactor system of the company Technobis. It includes the heating of stirred lignin dispersions with different ethanol contents and detection of agglomeration via turbidity measurement.

Pulping liquor was diluted with ultrapure water to form lignin dispersions with different ethanol mass fractions. The dispersions were mixed in 8 mL glass vials by magnetic stirring in the Crystalline reactor. The samples were heated from room temperature to a maximum of 95 °C at 0.5 K/min. Turbidity was measured by a red laser beam that radiated through the sample and was detected on the opposite side of the vial. At the same time, micrographs of the particles were recorded once a minute by a built-in microscope camera.

During the heating process, particles started to agglomerate at certain temperatures. Agglomeration was detected by turbidity measurement and the agglomeration temperature was defined at the temperature, at which the turbidity started to decrease or the transmissivity started to increase, respectively. Particle micrographs were additionally considered to ensure agglomeration really occurred.

**2.2.2.2. Continuous Precipitation and Agglomeration in Lab Plants.** The lab plant experiments have been carried out in two modifications of the plant shown in Figure 1. The first lab plant setup comprised heat-input via the double-jacket of a stirred reaction vessel. The optimized modification was equipped with a falling film evaporator for heating that significantly reduced foaming of the boiling lignin dispersion.

**Setup with Jacket Heating.** The setup for the continuous precipitation experiments with jacket heating is shown in Figure 1 (left). The plant mainly consisted of four differently colored subunits that are each characterized by the process



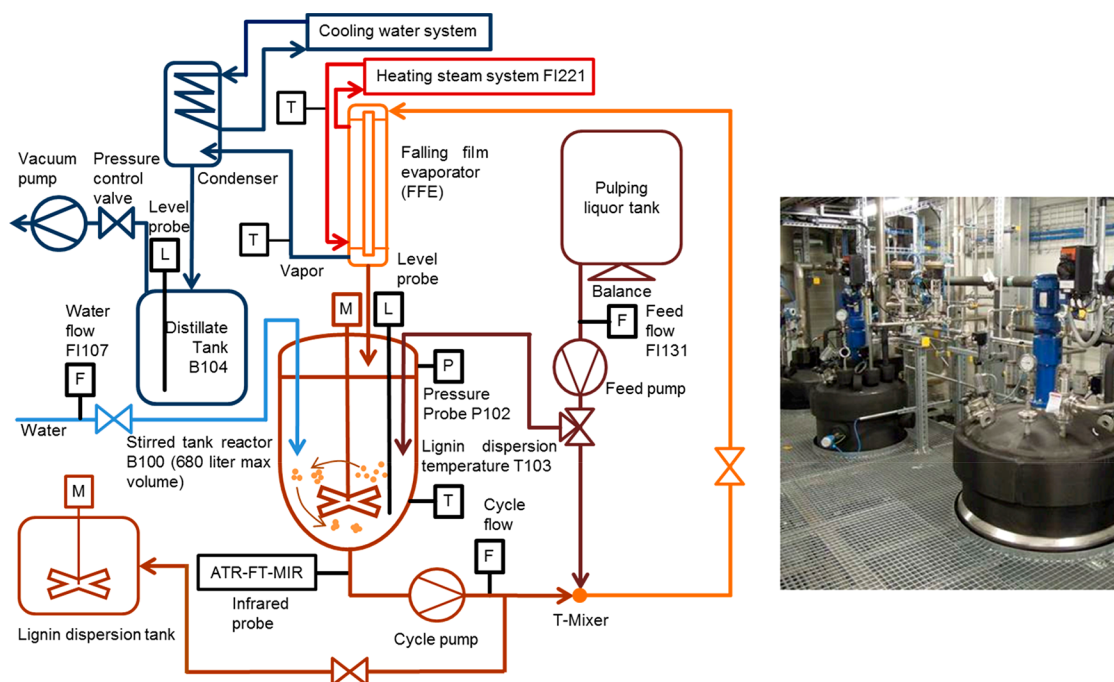


**Figure 2.** Left: Flowsheet of the pilot plant for continuous lignin precipitation. In comparison to the lab plant, the pilot plant is about a factor of 210 larger and has no distillation column. Therefore, an extra water feed was added. Water must be added to avoid excessive concentrations of solids, because relatively large amounts of water can evaporate together with the ethanol under adverse operation conditions. Right: Photograph of the upper parts of the 680 L stirred tank reactor and the dispersion tank on the second floor of the pilot plant.

stream they contain: (1) the 2 L pulping liquor tank and feed pump (brown), (2) the 2 L heated reactor (light brown), (3) the 1 L dispersion tank with dispersion removal pump (dark brown) and (4) the distillate (rectification column, condenser and 1 L distillate tank) and vacuum system (blue).

For start-up, about 1 kg of ultrapure water was mixed with pulping liquor to form the start-up dispersion with an ethanol content of around 8 wt %. Afterward, a constant heating power was supplied via the heating-thermostat (Lauda Proline RP845) that was regulating to a temperature around 10 K above the lignin dispersion temperature. The pulping liquor feed pump was started with around 3 to 4 g/min and was adjusted during the process to obtain ethanol contents around 7.5 wt % in dispersion, measured by the infrared probe (see in section 2.2.1). At nearly the same time the reflux valve was opened to withdraw distillate and the dispersion pump was started to remove dispersion from the reactor in order to maintain a constant dispersion level. The lignin precipitated continuously in the area of the feed pipe inlet because of the ethanol mass fraction drop during mixing with the dispersion in the reactor. Distillate and dispersion masses were recorded by balances to monitor the process mass balance at any time. The size distribution of lignin particles in the dispersion was monitored by the FBRM probe, lignin particle shape and agglomeration via the inline microscope. When the pulping liquor tank was emptied the experiment was stopped. The ethanol mass fraction of the distillate was determined by GC-headspace or density measurement. The ethanol mass fractions were derived from the correlation with the density. The continuously removed dispersion and the dispersion drained after the experiment from the reactor were both filtered in a pressure cake filtration setup to determine the average filter cake resistance.

*Setup with Falling Film Evaporator.* The continuous precipitation experiments with a falling film evaporator were carried out in the experimental setup shown in Figure 1, right. The setup distinguished from the setup with the jacket heating mainly in an additional lignin dispersion cycle powered by a gear pump to supply a constant flow for the falling film evaporator (orange parts in Figure 1, right). The infrared probe was removed from the reactor lid and installed in the new dispersion cycle. Additionally, as the minimum filling level of the reactor was lowered the residence time of the lignin dispersion in the reactor could thereby be decreased. Lignin particle agglomeration and changes in particle size distribution were thought to be able to be measured faster and better controlled due to the shortened residence time. The pulping liquor feed position was moved from the reactor to the dispersion cycle in upstream position to the falling film evaporator in order to have the possibility to tune the dilution ratio of fed pulping liquor and thereby the ethanol mass fraction in the dispersion before entering into the evaporator. The falling film evaporator was made of a vertically installed straight Liebig-cooler with a self-made liquid distributor on the top and an extension tube at the bottom to drain the dispersion from the evaporator cycle directly to the dispersion in the reactor, while preventing the dispersion flowing down the reactor lid, causing incrustations.

The experimental procedure for start-up and continuous operation of the plant was similar to the plant with jacket heating. The amount of water for the start-up dispersion could be reduced by 50 % and the pump for the evaporation cycle was started at a flow rate of 250–500 g/min after the water was filled into the reactor. All subsequent steps were similar to the description given above for the first.

*2.2.2.3. Continuous Precipitation and Agglomeration in the Pilot Plant.* Continuous pilot scale precipitation experi-

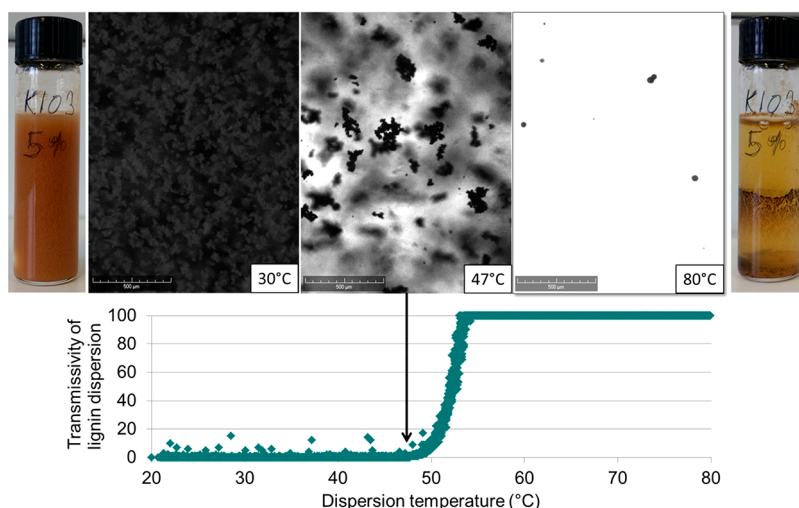


**Figure 3.** Typical result of an agglomeration temperature measurement carried out with a dispersion containing 0.25 wt % K103 lignin and 5 wt % ethanol. Top: Micrographs of dispersed lignin particles at increasing temperatures and photographs of vials with lignin dispersion before and after the experiment. The particles obviously agglomerate from a specific agglomeration temperature on. Bottom: Related transmissivity of the lignin dispersion as a function of temperature. Transmissivity increases rapidly beginning at the agglomeration temperature (here 47 °C).

ments with a falling film evaporator were carried out in the experimental setup shown in Figure 2. The pilot plant was upgraded on the basis of the results from the semicontinuous experiments that have been presented in previous work.<sup>30</sup> Therefore, a falling film evaporator with an accompanying dispersion cycle has been added to the plant. A rectification column was not installed, meaning that the ethanol/water vapor from the evaporator had to be directly condensed without ethanol enrichment. Therefore, an additional water feed was installed. Without the water-feed, the lignin dispersion could reach a too high solid-to-liquid content ratio, decreasing the mobility of the dispersion outlet stream. However, the reduction of the water feed to a lowest possible amount was a major goal in the experiments. Two pulping liquor feed positions, in the dispersion cycle and in the reactor, were installed to investigate their influence on the process. The dispersion removal valve was mounted in a way to allow continuously adjusting the reactor level and withdrawing lignin dispersion into the dispersion tank.

Furthermore, an infrared probe (ReactIR 45P with 9.5 mm AgX DiComp probe from Mettler Toledo) has been installed in the dispersion cycle in order to improve process control in terms of the ethanol content in the dispersion. Dispersion samples were additionally analyzed after the experiments with GC-hs. The ethanol content was measured every 30 s and the process could be tuned better. However, no FBRM and V19 probe were available for particle size and agglomeration monitoring. The particle size was estimated from the color and the sedimentation behavior of the dispersion during the experiment. Later samples of the lignin dispersion have been analyzed with the FBRM probe and lignin particles by light microscopy. The dry substance content of the lignin dispersion was measured gravimetrically (Infrared Moisture Analyzer, Sartorius) and the ethanol mass fraction of the distillate via density.

Suitable process conditions (feeds, heating, pressures, etc.) for the prevention of lignin fouling, etc. have been preliminary calculated for all experiments by a basic mathematical process model, which considers mass and energy balances and phase transitions in the pilot plant.<sup>31</sup>

The reactor was filled with around 220 kg of lignin dispersion by mixing K139 pulping liquor (see Table 1) with desalinated water. The dispersion was used as start-up dispersion and contained around 6 wt % ethanol in the aqueous phase. The pressure over the dispersion was regulated to 120 mbar, the evaporator cycle pump was started with a flow rate of 3500 kg/h and the heating steam was turned on to heat-up the system to evaporation conditions, while the distillate was completely refluxed. The pulping liquor feed pump was started with ~50 kg/h to obtain ethanol contents between 6 and 8 wt % in the dispersion. The desalinated water mass flow was regulated to 45 kg/h to compensate the removal of water by the distillate. The heating steam mass flow was regulated to 34 kg/h, which is equal to about 25 kW heating power. The lignin precipitated continuously at the feeding position in the reactor because of the ethanol mass fraction drop during mixing with the dispersion.

In order to find the lowest possible water feed rate, the water feed was stepwise reduced to zero throughout the experiments. The ethanol content and agglomeration behavior was assessed after each water reduction in order to prevent uncontrolled softening of lignin. Subsequently, the pulping liquor feed rate and heating steam flow were increased by 10% to check the operational limits of the plant. Dispersion and distillate samples have been taken regularly throughout the experiment and were analyzed by GC-headspace and FBRM afterward.

The experiment was stopped after the first day and continued on the next day. The process was terminated after the pulping liquor tank was emptied.

### 3. RESULTS

**3.1. Pulping Liquor Compositions and Lignin Properties.** The pulping liquors were investigated in terms of composition and lignin properties before they were processed.

Table 1 shows pulping conditions as well as lignin and ethanol contents of the liquors studied in this work. In most liquors the content of dissolved hemicellulose (sugars, not shown in the table) is almost the same as lignin.

Generally, the lignin contents are quite low and originate from the liquor-to-wood ratio in the pulping process. The

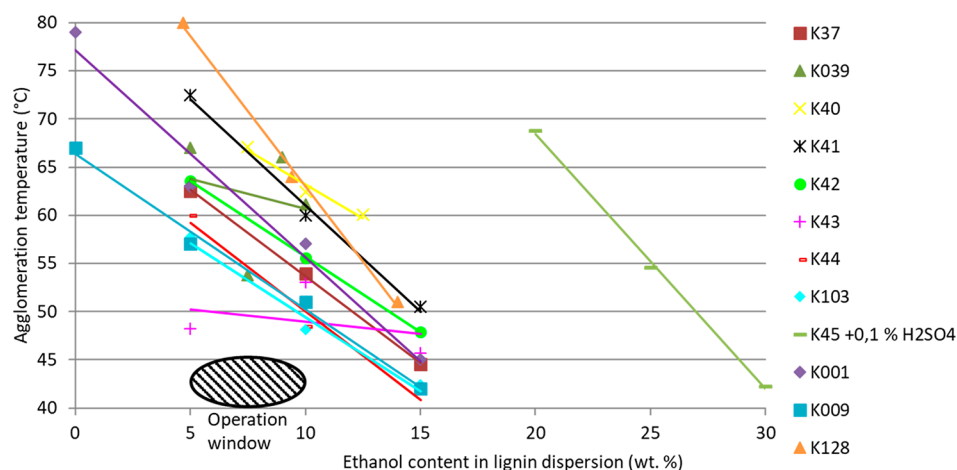


**Figure 4.** Agglomeration temperatures of investigated lignins/pulping liquors, depending on the ethanol content of the dispersion. The lines are fitted linear functions. The marked operation window illustrates the range of conditions for first continuous lignin precipitation experiments.

batch pulping is performed with a dry wood content of about 24 wt %. The subsequent washing step with almost the same amount of solvent reduces the overall wood in the pulping batch content to about 12 wt %. It can be estimated that approximately 15–25 wt % of lignin are dissolved from the wood, resulting in 1.8–3 wt % lignin content dissolved in the pulping liquor (spent + wash liquor).

The molecular masses of lignins investigated within this work have been measured by HPSEC and the results are listed in Table 1. The weight-average molar masses range between 1949 (K41) and 5868 (K45) g/mol. The distinct high value of K45 lignin was derived from a mild pulping batch resulting in significantly larger lignin molecules compared to the other lignins investigated. Overall, the molar masses are in a typical range for organosolv lignins.<sup>32,33</sup> The polydispersity, which is a measure for the broadness of molar mass distributions (i.e., equals 1 if all molecules have the same mass) ranges between 2.2 and 5.2. The results show that the polydispersity increases with the weight-average molar mass.

### 3.2. Softening and Agglomeration Temperatures.

Figure 3 shows a typical result of an agglomeration temperature measurement combining recorded micrographs and photographs (top) with corresponding transmissivities of the lignin dispersion as a function of the temperature (bottom). The first micrograph and photograph depict dispersed lignin particles in a vial at 30 °C. They appear gray-colored because they reflect the front light of the camera device and the back light is completely absorbed by the dispersed particles, so the background appears black. At 47 °C the particles appear black because the back light is not absorbed any more by the dispersed particles and the background appears now white. Obviously, the particles started to agglomerate. At 80 °C most of the particles deliquesced (melted) and appear as droplets. The amount of visible lignin is clearly lower because it sticks to the stirrer and the glass and is not dispersed any more (see photograph on the right).

The laser transmissivity through the dispersion (Figure 3, bottom) shows the onset of an increase at 47 °C that clearly corresponds to lignin agglomeration (see black arrow). This onset in increasing transmissivity was defined as agglomeration temperature and determined for the different lignins (liquors) studied.

Agglomeration requires lignin particles to form aggregates at first, so that the particles are in contact with each other. The aggregated particles can form solid bridges between each other if the particles are soft enough to form agglomerates. The aggregation of particles in dispersions is strongly influenced by the  $\zeta$ -potential, a measure for the electrostatic charging of the particles.<sup>34</sup> It should be noted that the  $\zeta$ -potential is strongly influenced by the pH value and ion strength of the liquid phase. At a  $\zeta$ -potential around zero, aggregates form easily and agglomeration can be observed immediately at the lignin softening temperature. If the  $\zeta$ -potential of a dispersion is around + or –30 mV, lignin particles do not aggregate and therefore also do not agglomerate by forming lignin bridges when approaching the softening temperature. In this case, agglomeration would not be observed even if the particles are softened already. For this reason, sulfuric acid had to be added to the K45 (see Table 1) lignin dispersions in order to decrease the  $\zeta$ -potential and allow particle agglomeration to identify the K45 lignin softening temperatures. The  $\zeta$ -potential of lignin dispersions has been reported in literature and showed significant dependence on the pH value.<sup>35,36</sup>

As presented in Figure 4, a linear dependency of the agglomeration temperature on the ethanol mass fraction in the dispersion was found for most lignins, except for K39 and K43. The slopes of the fitted linear functions range between –1.4 and –3.1 (°C/wt % ethanol). Ethanol has clearly different impacts on the softening of various lignins. Lignins with larger slopes in Figure 4 were more strongly softened by ethanol than those with lower slopes. Agglomeration occurs as result of lignin softening and formation of bridges between single lignin particles by coalescence or sintering, as already described in literature for lignin<sup>37</sup> and other systems.<sup>38</sup> Chemical properties of lignins that could correlate to the different slopes were not investigated within this work.

The partly extrapolated intersections of the fitted linear functions with the  $y$ -axes at 0 wt % ethanol, relating to the softening temperature in pure water, range from 65 to 121 °C, whereas the majority lies between 65 and 94 °C. Only K45, characterized by the highest molecular mass, would have been softened at 121 °C in pure water. K45 did not agglomerate below the boiling temperature of the dispersion when tested at ethanol contents that were used for the other lignins. So, the ethanol content had to be increased to decrease the



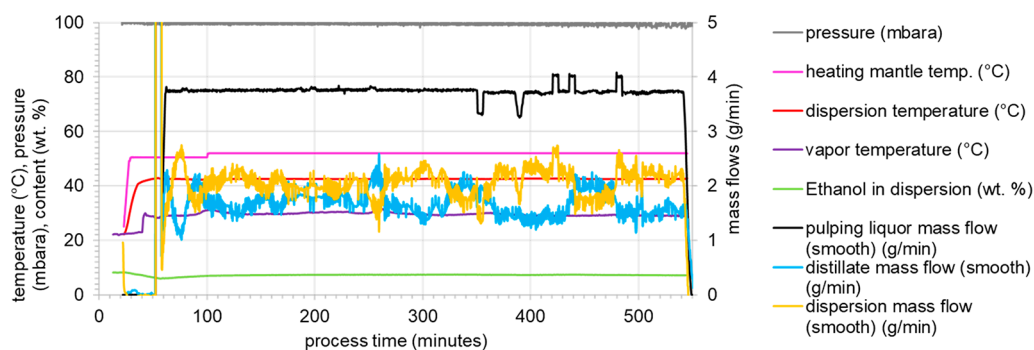


Figure 5. Process trends of relevant parameters of continuous precipitation of K40 pulping liquor.

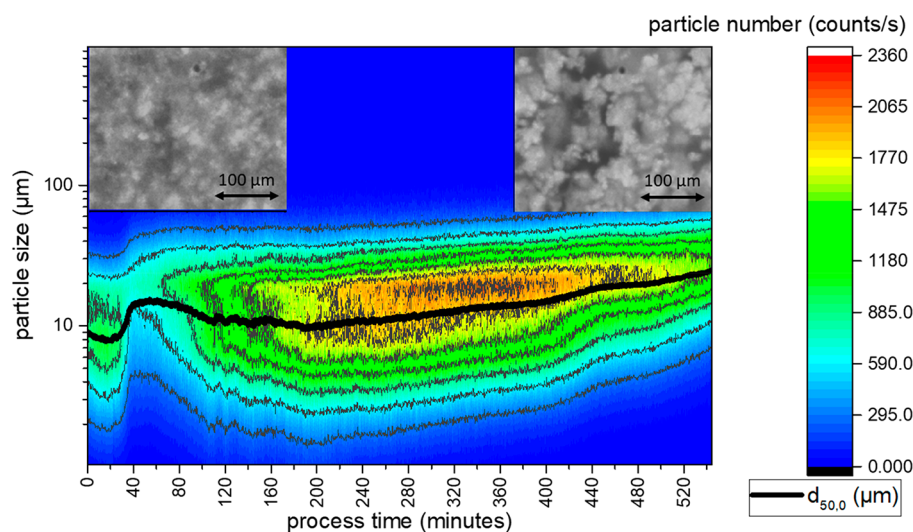


Figure 6. Particle size (chord length) number distribution of K40 lignin particles as contour plot during continuous precipitation. Two micrographs of lignin particles at the beginning and at the end of the experiment are shown above the contour plot.

agglomeration temperature. The results are still comparable because the same phenomenon (agglomeration) was observed. The decrease of the glass transition temperature of lignin by absorbed water has already been reported in literature.<sup>39</sup> The results in this work show that different lignins become softened by water to a different extent. Clear correlations between the softening temperatures in water and other lignin properties (e.g., glass transition temperatures<sup>31</sup>) were not found within this work. Continuing on, K45 lignin was found to have a significantly higher softening temperature in water and has by far the highest molar mass of the investigated lignins. It is well-known in polymer science that glass transition and softening temperatures of polymers increase with increasing molar mass of the polymer and swellability is decreased with increasing polymer molar mass.<sup>40</sup> However, it is assumed that the molar mass range of the investigated lignins is too small to elucidate correlations to the softening properties.

Based on the results of the agglomeration behavior studies, the operation window for the continuous lignin precipitation experiments from organosolv pulping liquors was derived. It is indicated in Figure 4 at a temperature of 40–45 °C and an ethanol content in the lignin dispersion of 5–10 wt % and is located in the region of “hard” lignin in order to prevent uncontrolled lignin softening and fouling during the process.

**3.3. Continuous Precipitation and Agglomeration.** The experiments have been carried out in two modifications of a lab plant and in the reconstructed pilot plant at Fraunhofer

CBP as described in sections 2.2.2.2 and 2.2.2.3. Numerous experiments were performed, but only typical experimental results are presented in this section. A list of the performed experiments is given in Table S1.

**3.3.1. Lab Plant with Jacket Heating.** In total ten different pulping liquors were processed within the 24 experiments in this setup. Here, the results of the continuous precipitation of K40 pulping liquor, that showed similar behavior like the other processed liquors, are discussed in comparison to that of K45, that showed clearly different behavior. Both liquors were produced from beech wood and at relatively low temperatures (170 °C) but K40 with and K45 without sulfuric acid addition to the pulping solution.

The most important process parameter trends of K40 precipitation are plotted over process time in Figure 5. Shown are relevant temperatures, pressure and ethanol content on the left y-axis as well as mass flows on the right y-axis. As can be seen in the trends the start-up dispersion (red line) was heated up by the heating medium (magenta line) to boiling temperature (43 °C) and the rectification column head temperature was equilibrated (violet line) at total reflux until the 60th minute. The pressure (gray line) was held constant at 100 mbar. The pulping liquor feed (black line) was started in the 60th minute and adjusted to about 3.7 g/min during the whole experiment. The distillate flow (blue line) was controlled by the reflux valve, which was in turn manually adjusted in order to keep the vapor temperature (violet line) at

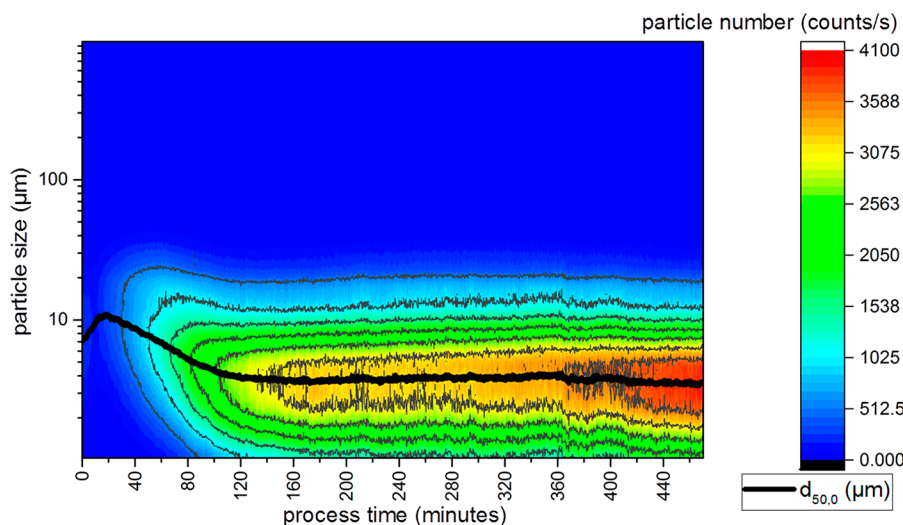


**Figure 7.** Particle size (chord length) number distribution of K45 lignin particles as contour plot during continuous precipitation. Contrary to K40 lignin, the K45 lignin did not agglomerate at all. This behavior corresponds to the high agglomeration temperatures measured for K45 lignin.

the head of the distillation column close to the azeotropic temperature. The dispersion flow (yellow line) was also manually controlled in order to keep the dispersion level in the reactor constant. The ethanol content (green line) was adjusted within the range of 7 to 8 wt % by tuning the heating jacket temperature (magenta line) or the pulping liquor feed. After about 550 min the pulping liquor tank was depleted and the experiment was stopped.

Figure 6 shows the particle size number distribution (PSD) of K40 particles over the process time as a contour plot and two micrographs of lignin particles recorded with the inline microscope at the beginning and end of the experiment, respectively. During the heating-up phase, around the 40th minute the lignin particles of the start-up dispersion agglomerated. The  $d_{50,0}$  (median) increased from  $\approx 8$  to 15  $\mu\text{m}$  and the overall particle number decreased. When the pulping liquor feed was started at the 60th minutes, the median decreased again to 10  $\mu\text{m}$  and the particle counts  $< 10 \mu\text{m}$  increased because of the addition of freshly precipitated small lignin particles to the population. The trend to smaller particles stopped after 200 min and the PSD started to drift to bigger particle sizes until the end of the experiment. In particular particles below 10  $\mu\text{m}$  almost completely disappeared until the experiments end because they were probably incorporated in larger agglomerates. The micrographs support the observations of the FBRM signal, as they clearly show larger agglomerates at the end of the process when compared to particles at the beginning.

This observed drift of particle size number distribution during the continuous precipitation process has been obtained in the major part of conducted experiments, except K45.

No experiment reached the steady-state in terms of dispersion composition, and therefore, the start-up to steady period has been followed in every experiment. The mean residence time  $\tau$  of the lignin dispersion in the continuous stirred-tank reactor (CSTR) can be described by  $\tau = m_{\text{disp}} / \dot{m}_{\text{disp}} = 1300 \text{ g} / (2 \text{ g/min}) = 650 \text{ min}$ , with  $m_{\text{disp}}$ : mass of dispersion in the reactor and  $\dot{m}_{\text{disp}}$ : mass flow of dispersion. Steady-state would have been reached after about 3 to 4 mean residence times (3 to 4 times 650 min) when assuming the behavior as continuous stirred-tank reactor (CSTR). Thus, all experiments have been observed during the first quarter of the start-up

phase to steady-state. Consequently, the dispersed lignin content of the dispersion and the sugar and acid contents in the aqueous phase of the dispersion increased during the whole experiment. Accordingly, the pH value decreased and the dissolved metal salt concentration (originating from wood and reactors) increased as result of the reduced water content. Thus, the  $\zeta$ -potential of lignin particles may get closer to zero by the positively charged ions which correspondingly increases the agglomeration rate. An increasing agglomeration rate throughout the experiment could explain the observations regarding the PSD. The lignin particles were agglomerating right from the beginning but the nucleation rate was higher at the time the feed was started through the time that the PSD decreased at first. After some time the agglomeration rate surpassed the nucleation rate and the PSD drifted to larger particle sizes. The nucleation rate is assumed to stay practically constant because the feed flow was also nearly constant during the experiments.

The conclusion here is that the agglomeration rate would increase until the steady-state composition of the lignin dispersion is reached. Of course, the agglomeration rate will not linearly increase because the ion and acid concentrations will not linearly increase, and the  $\zeta$ -potential and pH value do not linearly change with acid content and ion strength either. However, when getting closer to the steady-state dispersion composition, it would be necessary to adjust the agglomeration rate by tuning the ethanol content or the dispersion temperature in order to prevent uncontrolled agglomeration and formation of lumps.

Contrary to the other processed pulping liquors, K45 did not agglomerate or aggregate. A small amount of sulfuric acid had to be added to the K45 lignin dispersion to enable agglomeration by lowering the  $\zeta$ -Potential of the dispersed particles. Additionally, K45 lignin agglomerated at significantly higher ethanol contents than the other investigated lignins (see section 3.2).

The K45 pulping liquor was processed at the same process conditions like K40 but in the pulping process no sulfuric acid was added. The evolution of the PSD over process time is shown in Figure 7. The median particle size decreased at the beginning of the precipitation process and remained at 3  $\mu\text{m}$  until the end of the experiment. The K45 particles did not



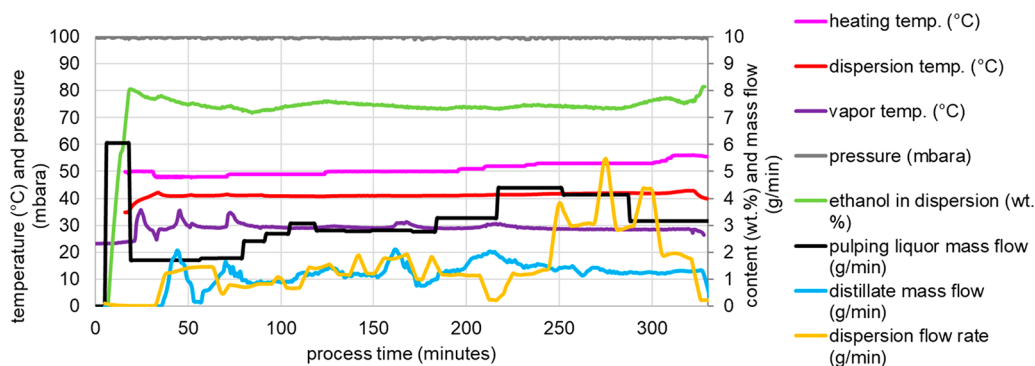


**Figure 8.** Process trends of relevant parameters of continuous precipitation of K128/1 pulping liquor in the lab plant with falling film evaporator.

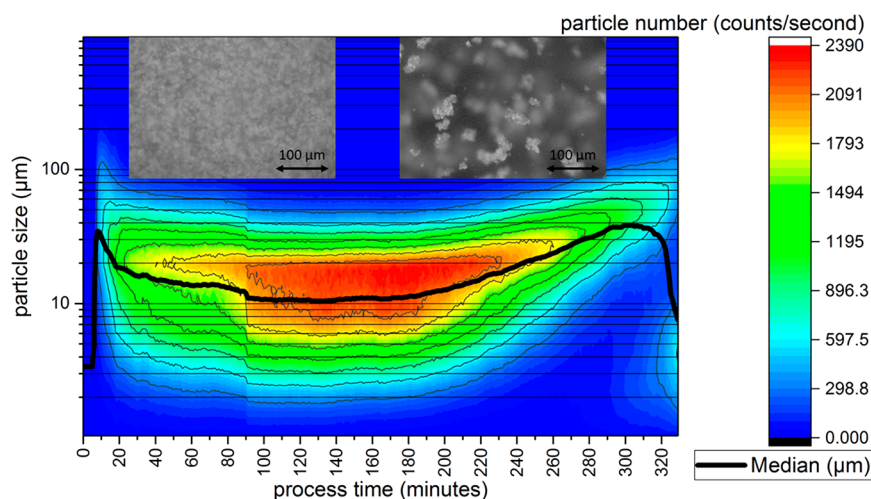


**Figure 9.** Particle size (chord length) number distribution of K128/1 lignin particles as contour plot during continuous precipitation. Two micrographs of lignin particles at the beginning and at end of the experiment are shown above the contour plot. Significant agglomeration correlates with elevated heating temperature in the falling film evaporator.

agglomerate at all. This behavior correlates to the agglomeration properties of K45 because it agglomerates at significant higher temperatures and ethanol contents than the other lignins (Figure 4). Consequently, the K45 lignin was not soft during the process and therefore did not agglomerate. Additionally, even no particles aggregates were observed, what might be caused by a high  $\zeta$ -potential of the particles.

The average filter cake resistance of the produced lignin dispersions was measured to quantify the achieved filterability. The experiments were carried out in a self-constructed pressure filter setup. The average filter cake resistance was calculated applying the modified CARMAN equation, as described in literature.<sup>41,42</sup> Good filterability (values in the region of  $10^{11} \text{ m}^{-2}$  and  $10^{12} \text{ m}^{-2}$ ) were determined for the agglomerated lignins K37 to K44. The not agglomerated K45 lignin dispersion was practically not filterable (average filter cake resistance of about  $10^{17} \text{ m}^{-2}$ ). These results show that particle agglomeration is mandatory to achieve a good filterability, what is especially important for scaling-up of the precipitation process.

An undesired effect of lignin agglomeration in this experimental setup was expressed by the low lignin yields of 52–85 wt % that were achieved for the lignins K37 to K44. They correspond to the agglomeration because soft lignin enriched in the foam above the boiling dispersion and formed incrustations on the warm reactor wall and on the analytical probes. The incrustated lignin is not contained in the lignin yield

(=dry mass of lignin filter cake/mass of fed pulping liquor/lignin content in pulping liquor  $\times$  100%) and therefore the yield is also a measure for the incrustations. The yield of K45 lignin could not be determined as the dispersion was not filterable but visually no incrustation was observed. So, a yield close to 100% can be assumed.

The results clearly show that a trade-off between agglomeration and yield has to be made because agglomeration requires softening of lignin first and the soft lignin can form incrustations that lower the yield. However, foam-boiling of the dispersion contributed significantly to the formation of incrustations. This was the reason to upgrade the plant by a falling film evaporator that should prevent foaming.

**3.3.2. Lab Plant with Falling Film Evaporator (FFE).** The results of two experiments with K128 pulping liquor from eucalyptus wood are presented in this section (K128/1 and K128/3). The results show that relatively small changes in the operation conditions (pressure, temperature and ethanol content) clearly influence the lignin particle agglomeration.

Figure 8 shows trends of some process parameters of experiment K128/1. The pressure (gray), ethanol content of the dispersion (green) and temperature of the dispersion (red) were adjusted to 100 mbar, 7–8 wt % and  $\approx 41 \text{ }^\circ\text{C}$ , respectively. The heating medium temperature in the FFE (magenta) and the flow rate of pulping liquor (black) have been increased during the experiment from 49 to 56  $^\circ\text{C}$  and from 1.8 to 4.3 g/min, respectively.

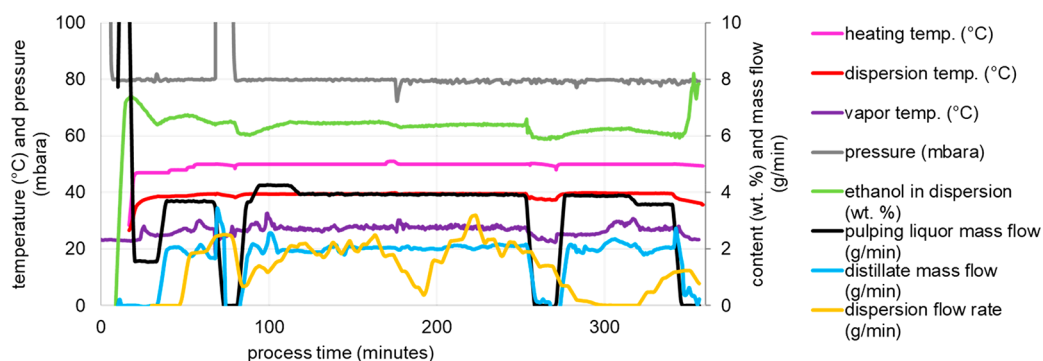


**Figure 10.** Process trends of parameters of continuous precipitation of K128/3 pulping liquor in the lab plant with falling film evaporator under milder operation conditions compared to those given in Figure 8.

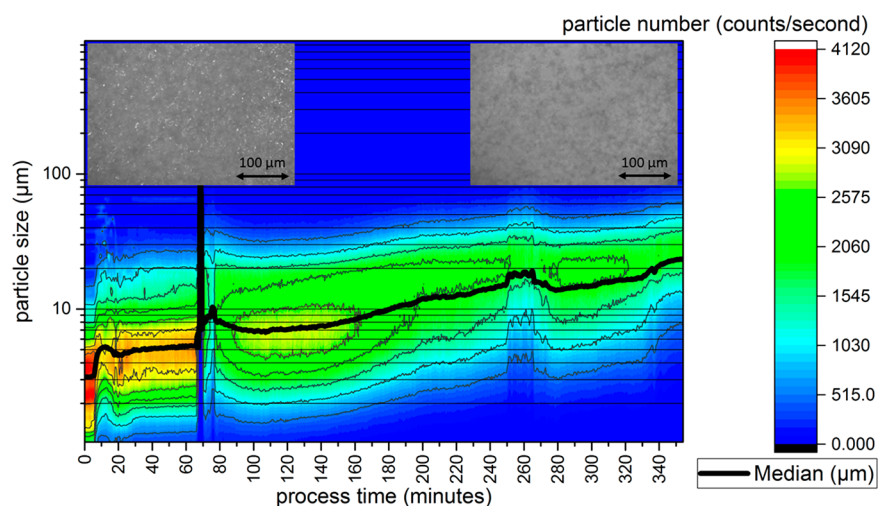


**Figure 11.** Particle size (chord length) distribution of K128/3 lignin particles as contour plot during continuous precipitation under milder process conditions. The step down of the median around the 270th minute was caused by a technical problem. Two micrographs of lignin particles at the beginning and at the end of the experiment are shown above the contour plot.

The corresponding development of the particle size number distribution (PSD) over process time is plotted in Figure 9. The median particle size first decreased from  $\approx 30$  to  $10 \mu\text{m}$  during the first 180 min. Then agglomeration became more prominent and the median particle size increased to  $40 \mu\text{m}$  until the 300th minute. This agglomeration may have been triggered by the increase of the heating temperature of the FFE above a critical value at the given operation parameters. Subsequently, around minute 320, the disappearance of the agglomerated fraction sized between 20 to  $100 \mu\text{m}$  and the appearance of a new fraction of small nuclei sized between 1 to  $10 \mu\text{m}$  was measured.

The micrographs of the lignin particles (Figure 9) also clearly show the extent of agglomeration and support the information provided by the FBRM probe.

The sudden “disappearance” of the agglomerated particle fraction between minutes 300 and 320 can most likely be explained by sedimentation and incrustation of soft lignin.

The average filter cake resistance of  $1.2 \times 10^{13} \text{ m}^{-2}$  measured by pressure cake filtration (see Figure S1) proves a satisfactory filterability of the lignin dispersion. The dry lignin yield after filtration was only 59 wt % of the theoretical value. The corresponding loss of 41 wt % lignin in incrustation supports the explanation given above.

Accordingly, the operation conditions for the next experiment with the same pulping liquor (K128/3) were adjusted to lower temperature and ethanol content.

Temperatures of the FFE heating medium and the dispersion and ethanol contents have been lowered in relation to the K128/1 run to decrease losses of lignin in incrustations. Figure 10 shows the resulting trends of process parameters. The pressure, ethanol content of the dispersion, temperature of the dispersion and heating medium temperature in the FFE were adjusted to 80 mbar, 6–7 wt %,  $\approx 40$  and  $50 \text{ }^\circ\text{C}$ , respectively. The flow rate of pulping liquor was adjusted to 4 g/min and was stopped two times in the experiment because of technical problems.

The corresponding development of the lignin PSD over the process time is plotted in Figure 11. Once the FBRM probe was cleaned around the 70th minute, the measurement shows a slow agglomeration of the particles until the end of the experiment, reaching a median particle size of about  $25 \mu\text{m}$ . The micrographs in Figure 11 reveal almost the same particle sizes at the beginning and end of the process and support the results of the FBRM probe that showed moderate agglomeration.

Thus, agglomeration was clearly reduced compared to results shown in Figure 9 because of the slightly milder process conditions. The average filter cake resistance of the lignin dispersion was  $1.7 \times 10^{13} \text{ m}^{-2}$  (see Figure S1) again

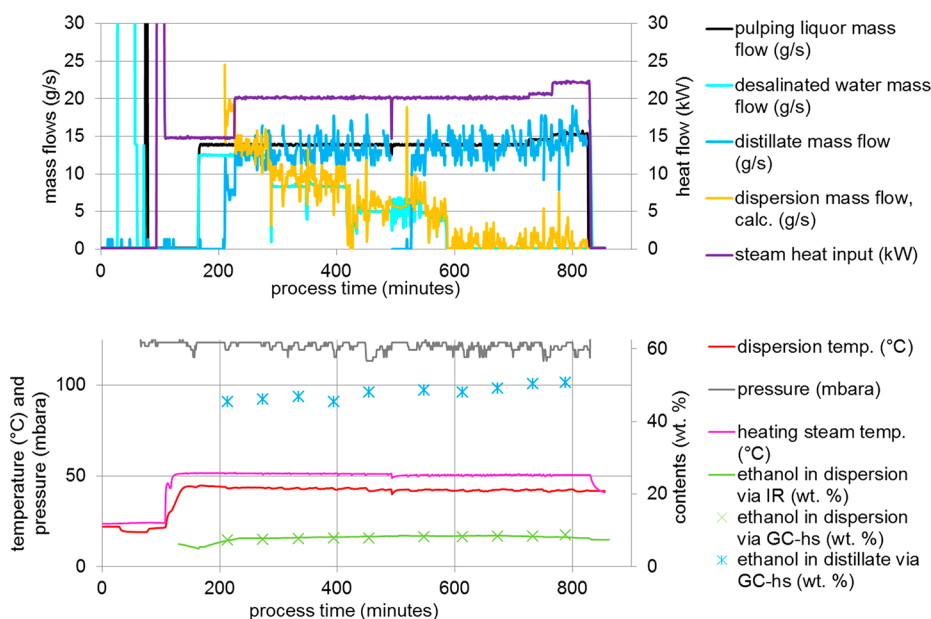


**Figure 12.** Top: Process parameter trends of important mass and heat flows of two subsequent pilot-scale experiments for continuous precipitation of K139 lignin. Bottom: Pressure, temperatures and ethanol contents as a function of process time (both plots share the same time axis). Ethanol contents in dispersion were measured twice, by an inline infrared probe and an offline GC-headspace. Ethanol contents in the distillate were simply measured by GC-headspace.

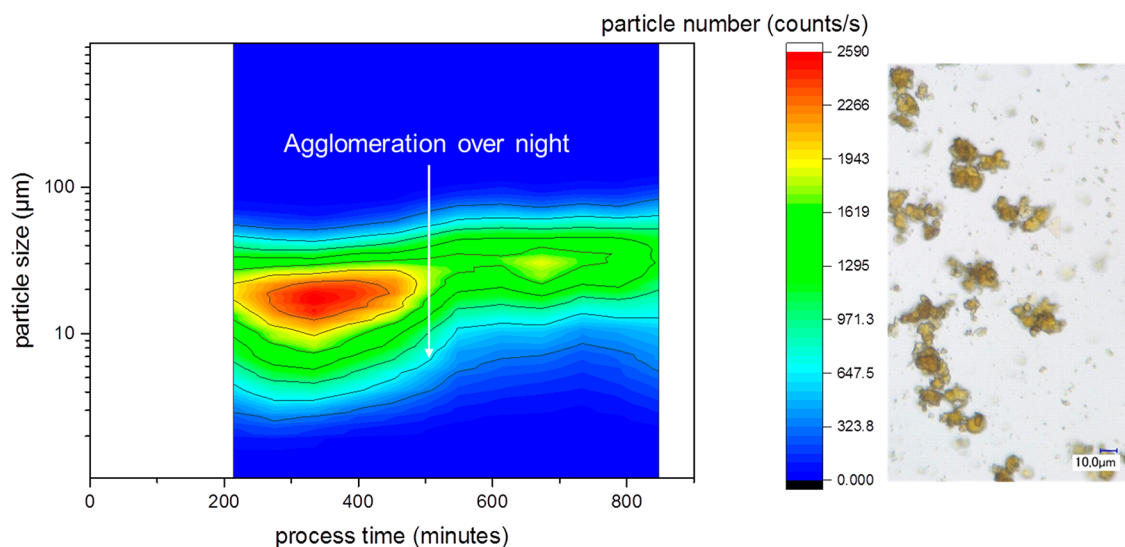


**Figure 13.** Left: PSD of K139 particles over the process time of two subsequent days (during daylight hours only). Agglomeration occurred mainly during the night between the two experimental days. Right: Micrograph of lignin particles at the end of the experiments. Mainly agglomerates (10–20 μm) and some primary lignin particles (1–2 μm) are observable.

verifying a satisfactory filterability. Even though the lignin particles agglomerated less than in the previous experiment the filterability is still in the same range. As result of the adapted conditions the dry lignin yield found was 99 wt % and correlates to the complete prevention of incrustation formation.

The agglomeration rate in this experiment K128/3 could be regulated to a moderate level compared to the first run K128/1 by lowering the heating temperature of the FFE, the temperature of the dispersion and the ethanol content in the dispersion, what resulted in less softening of the lignin particles. The operation conditions were still in the operation window illustrated in Figure 4 but in its lower end. The FFE temperature is assumed to have the largest influence on the

agglomeration behavior in this experiment because strong agglomeration started in the K128/1 trial when the heating temperature in the FFE exceeded 50 °C.

**3.3.3. Pilot Plant Trials.** Two experiments on two subsequent days have been carried out with K139 pulping liquor from beech wood. The process parameter trends are plotted in Figure 12. The first experiment ended after 492 min and the second experiment was started on the next day with the lignin dispersion of the day before. The start-up procedure of the second day was removed from the diagram.

Pressure (gray), ethanol content of the dispersion (green), temperature of the dispersion (red) and heating steam temperature in the FFE (magenta) were adjusted to 120 mbar, 6–9 wt %, 40–41 and 50 °C, respectively. The flow rate



of pulping liquor (black) was adjusted to 13.9 g/s (50 kg/h) and was increased to 15 g/s (54 kg/h) in the end. The water flow (cyan) was lowered in order to reduce the undesired dilution of the dispersion while the dispersion flow (yellow) was aimed not to decrease to zero because then the operation mode would switch to semicontinuous (fed-batch) and the dispersion density (mass fraction of dispersed solids) could become too high to maintain flowability of the lignin dispersion. Consequently, the dispersion flow was also markedly lowered to averagely 0.4 g/s and the ethanol content in the dispersion slightly increased to nearly 9 wt %. The increased ethanol content in the dispersion caused higher ethanol content in the vapor and distillate (blue) according to the vapor–liquid equilibria of ethanol and water. In this way, less water was removed from the dispersion by evaporation than was added with the pulping liquor. Consequently, a dispersion outflow could be maintained even without additional water feed.

The PSD over process time is illustrated as a contour plot in Figure 13. The dispersion samples have been investigated with the FBRM probe four days after the experiment assuming that the particles did not change during the storage at room temperature. At 23 °C no significant agglomeration occurs within some days, as the lignin is not soft enough. The PSD first shifted to smaller sizes and then to larger sizes from the 300th minute on. Between both experiments (around minute 500) the dispersion was stirred overnight between 40 and 43 °C (not shown here) and the particles agglomerated. Thus, the figure shows a step-like increase in particle size between 500 and 600 min. Afterwards the PSD experienced only minor changes.

The dry lignin yield achieved was  $101.5 \pm 7.7$  wt % (relative error mainly originates from relative errors of the lignin mass fraction in pulping liquor ( $\pm 7.4$  wt %)). Thus, practically 100% yield can be assumed because no lignin incrustations were observed in the plant and therefore the precipitated lignin was completely recovered as particulate phase. For filtration a chamber filter press was used. Unfortunately, the average filter cake resistance could not be measured in the pilot plant but the filterability was subjectively judged as “good” by the pilot plant operators.

The results show that even at 120 mbar, 43 °C dispersion temperature and nearly 9 wt % of ethanol in the dispersion, the lignin particles did not agglomerate too much and also no incrustations were formed, while the same parameters probably would have led to incrustations in the lab plant. Consequently, upscaling from lab to pilot scale influenced also the agglomeration and/or softening behavior of lignin. A possible explanation is the much higher irrigation density of the pilot plant's falling film evaporator ( $3 \text{ m}^3/\text{m/h}$ ) in comparison to the falling film evaporator in lab scale ( $0.5 \text{ m}^3/\text{m/h}$ ). A higher irrigation density avoids local overheating of the dispersion at the tube surface. It is reasonable to assume that local overheating of dispersion and lignin particles at the tube surface can cause lignin softening and enhances agglomeration.

It should be noted here that the pilot plant trials were planned with the help of a basic mathematical process model, which considers mass and energy balances and phase transitions in the pilot plant.<sup>31</sup> The predicted process trends fit well to the experimental data (see Figure S2 and Figure S3 in Supporting Information) what makes the model a valuable tool for further process planning and optimization.

## 4. CONCLUSIONS

A continuous lab-scale process for lignin precipitation was developed based on knowledge acquired from studying semicontinuous processing.<sup>30</sup> Additionally, softening and agglomeration of particulate lignin in aqueous dispersions with different ethanol contents have been studied to determine conditions (temperatures and ethanol contents) where lignins tend to soften/agglomerate and to form incrustations.

The continuous lab plant was equipped with inline particle analytics and ethanol content monitoring for process control. Particle agglomeration occurred after a certain process time although the temperature and ethanol content in the dispersion were below the lignin softening limits determined before. It was assumed that the lignin particles got softened on the warm heating jacket or in a foam with higher ethanol vapor content that was generated by bubble boiling. Additionally, the boiling foam caused lignin incrustations above the dispersion liquid level.

For those reasons the continuous lab plant was upgraded with a falling film evaporator (FFE) to prevent foaming of the lignin dispersion. With this final experimental setup, incrustations could be completely prevented. Lignin yields close to 100% have been achieved and dispersions of good filterability were produced by controlled agglomeration of lignin particles. Hereby, the agglomeration could be controlled by the heating-medium temperature of the FFE.

The FFE process setup was scaled-up by a factor of 210 (with respect to pulping liquor feed) from lab to pilot plant level but due to constructional restrictions without a rectification column and therefore with an additional (undesired) water feed. The larger scale and different operating conditions of the FFE caused less agglomeration of lignin particles and therefore allowed the process to operate at slightly higher temperatures and ethanol contents compared to the lab scale process. Because of the higher ethanol content in the dispersion, it was possible to avoid the feeding of water. To maintain continuous operation the ethanol content in the distillate has to be higher than in the pulping liquor. Thus, more pulping liquor has to be added than distillate is removed.

Incrustations could be completely prevented and the lignin yields reached practically 100%, while the achieved filterabilities were between good and satisfactory.

The ethanol cycle could be closed but a small portion of the ethanol still has to be separated from the aqueous hemi-cellulose solution after lignin filtration, what was not performed here.

We believe that the patented process “LigniSep” brings the concept of lignocellulose biorefinery closer to commercialization because it offers full lignin and solvent recovery, continuous operation and good filterability of the generated lignin particles.<sup>29</sup>

**Outlook.** Currently, the authors study within the European project “UNRAVEL” the applicability of the “LigniSep” process to acetone–water solvent systems generated by the FABIOLA process<sup>43</sup>.

## ■ ASSOCIATED CONTENT

### 📄 Supporting Information

The Supporting Information is available free of charge on the ACS Publications website at DOI: 10.1021/acs.iecr.8b04736.

List of conducted continuous lignin precipitation experiments; filtration functions of K128/1 and K128/

3 experiments used to calculate the average filter cake resistances; pilot plant trials (K138) process trends compared to trends predicted by a mathematical process model that was applied for planning of the process trials (PDF)

## AUTHOR INFORMATION

### Corresponding Author

\*P. Schulze. E-mail: [schulzep@mpi-magdeburg.mpg.de](mailto:schulzep@mpi-magdeburg.mpg.de). Phone: 0049 391 6110 323.

### ORCID

Peter Schulze: [0000-0002-1089-746X](https://orcid.org/0000-0002-1089-746X)

Andreas Seidel-Morgenstern: [0000-0001-7658-7643](https://orcid.org/0000-0001-7658-7643)

Heike Lorenz: [0000-0001-7608-0092](https://orcid.org/0000-0001-7608-0092)

### Notes

The authors declare no competing financial interest.

## ACKNOWLEDGMENTS

We thank the German Federal Ministry for Education and Research (BMBF) for financial support of Fraunhofer CBP within the projects "Biomasseaufschluss" (FKZ 031A454A) and "KomBiChemPro" (FKZ 031B0083A) where we have been incorporated as subcontractors of the Fraunhofer CBP.

## REFERENCES

- (1) *Fachagentur Nachwachsende Rohstoffe Roadmap Bioaffinerien*. BMELV, BMBF, BMU, BMWi: Gülzow, 2012.
- (2) Michels, J.; Wagemann, K. The German Lignocellulose Feedstock Biorefinery Project. *Biofuels, Bioprod. Biorefin.* **2010**, *4* (3), 263–267.
- (3) Cazacu, G.; Capraru, M.; Popa, V. I. Advances Concerning Lignin Utilization in New Materials. In *Advanced Structured Materials*, Thomas, S., Ed.; Springer: Berlin-Heidelberg, 2013; Vol. 18, pp 255–312.
- (4) Öhman, F. Precipitation and Separation of Lignin from Kraft Black Liquor. Doctoral thesis, Chalmers University of Technology, Göteborg, 2006.
- (5) Zhu, W. Equilibrium of Lignin Precipitation- the Effects of Ph, Temperature, Ion Strength and Wood Origins. Licentiate Engineering thesis, Chalmers University of Technology, Gothenburg, 2013.
- (6) Zhu, W. Z.; Theliander, H. Precipitation of Lignin from Softwood Black Liquor: An Investigation of the Equilibrium and Molecular Properties of Lignin. *BioResources* **2014**, *10* (1), 1696–1714.
- (7) Kouisni, L.; Gagne, A.; Maki, K.; Holt-Hindle, P.; Paleologou, M. Lignoforce System for the Recovery of Lignin from Black Liquor: Feedstock Options, Odor Profile, and Product Characterization. *ACS Sustainable Chem. Eng.* **2016**, *4* (10), 5152–5159.
- (8) Zakzeski, J.; Bruijninx, P. C.; Jongerijs, A. L.; Weckhuysen, B. M. The Catalytic Valorization of Lignin for the Production of Renewable Chemicals. *Chem. Rev.* **2010**, *110* (6), 3552–99.
- (9) Strassberger, Z.; Tanase, S.; Rothenberg, G. The Pros and Cons of Lignin Valorisation in an Integrated Biorefinery. *RSC Adv.* **2014**, *4* (48), 25310–25318.
- (10) Menon, V.; Rao, M. Trends in Bioconversion of Lignocellulose: Biofuels, Platform Chemicals & biorefinery Concept. *Prog. Energy Combust. Sci.* **2012**, *38* (4), 522–550.
- (11) Viell, J.; Harwardt, A.; Seiler, J.; Marquardt, W. Is Biomass Fractionation by Organosolv-Like Processes Economically Viable? A Conceptual Design Study. *Bioresour. Technol.* **2013**, *150*, 89–97.
- (12) Vishtal, A. G.; Kraslawski, A. Challenges in Industrial Applications of Technical Lignins. *BioResources* **2011**, *6* (3), 3547–3568.
- (13) Tayenthal, K.; Kleinert, T. Process of Decomposing Vegetable Fibrous Matter for the Purpose of the Simultaneous Recovery Both of the Cellulose and of the Incrusting Ingredients. Patent US1856567 (A), 1932.
- (14) Kleinert, T. Organosolv Pulping and Recovery Process. Patent US3585104 (A), 1971.
- (15) Botello, J. I.; Gilarranz, M. A.; Rodriguez, F.; Oliet, M. Recovery of Solvent and by-Products from Organosolv Black Liquor. *Sep. Sci. Technol.* **1999**, *34* (12), 2431–2445.
- (16) Thring, R. W.; Chornet, E.; Overend, R. P. Recovery of a Solvolytic Lignin: Effects of Spent Liquor/Acid Volume Ratio, Acid Concentration and Temperature. *Biomass* **1990**, *23* (4), 289–305.
- (17) Hallberg, C.; O'Connor, D.; Rushton, M.; Pye, E. K.; Gjennestad, G.; Berlin, A.; MacLachlan, J. R. Modular System for Organosolv Fractionation of Lignocellulosic Feedstock. Patent US8528463 B2, 2013.
- (18) Alriols, M. G.; García, A.; Llano-ponte, R.; Labidi, J. Combined Organosolv and Ultrafiltration Lignocellulosic Biorefinery Process. *Chem. Eng. J.* **2010**, *157* (1), 113–120.
- (19) Weinwurm, F.; Drljio, A.; Silva, T. L. S.; Friedl, A. Principles of Ethanol Organosolv Lignin Precipitation: Process Simulation and Energy Demand. *Chem. Eng. Trans.* **2014**, *39*, 583–588.
- (20) Le, H. Q.; Pokki, J. P.; Borrega, M.; Uusi-Kyyny, P.; Alopaus, V.; Sixta, H. Chemical Recovery of Gamma-Valerolactone/Water Biorefinery. *Ind. Eng. Chem. Res.* **2018**, *57* (44), 15147–15158.
- (21) Huijgen, W. J. J.; Reith, J. H.; den Uil, H. Pretreatment and Fractionation of Wheat Straw by an Acetone-Based Organosolv Process. *Ind. Eng. Chem. Res.* **2010**, *49* (20), 10132–10140.
- (22) Macfarlane, A. L.; Prestidge, R.; Farid, M. M.; Chen, J. J. Dissolved Air Flotation: A Novel Approach to Recovery of Organosolv Lignin. *Chem. Eng. J.* **2009**, *148* (1), 15–19.
- (23) Michels, J.; Imami, A.; Stücker, A.; Duwe, A.; Susanto, A.; Saake, B.; Meier, D.; Küstermann, E.; Fliedner, E.; Meier, E.; Unkelbach, G.; Zorn, H.; Kühnel, I.; Podschun, J.; Strüven, J.-O.; Schweinle, J.; Becker, K.; Ziegler, L.; Fröhling, M.; Amann, M.; Naundorf, M.; Haase, M.; Leschinsky, M.; Tippkötter, N.; Engel, P.; Schweppe, R.; Lehnen, R.; Böringer, S.; Laure, S.; Riemer, S.; Zibek, S.; Sieker, T.; Pohsner, U.; Bäcker, W. "Lignocellulose-Bioraffinerie" *Aufschluss Lignocellulosehaltiger Rohstoffe Und Vollständige Stoffliche Nutzung Der Komponenten (Phase 2). Final Report, Fkz: 22029508, 22019009, 22019109, 22019209, 22019309, 22019409, 22019509, 22019609, 22019709, 22019809, 22019909, 22020009, 22020109, 22020209, 22022109; 2014.*
- (24) Pye, E. Integrated Processing of Biomass and Liquid Effluents. Patent US 2002/0069987 A1, 2002.
- (25) Berlin, A.; Balakshin, M. Y.; Ma, R.; Gutman, V. M.; Ortiz, D. Organosolv Process. Patent US 20130210100 A1, 2013.
- (26) Diebold, V. B.; Cowan, W. F.; Walsh, J. K. Solvent Pulping Process. Patent US 4100016 A, 1978.
- (27) Bouxin, F. P.; Jackson, S. D.; Jarvis, M. C. Organosolv Pretreatment of Sitka Spruce Wood: Conversion of Hemicelluloses to Ethyl Glycosides. *Bioresour. Technol.* **2014**, *151*, 441–444.
- (28) Sharazi, A. M.; van Heiningen, A. Ethyl Xylosides Formation in Sew (Avap (R)) Fractionation of Sugarcane Straw; Implications for Ethanol and Xylose Recovery. *Holzforschung* **2017**, *71* (12), 951–959.
- (29) Schulze, P.; Lorenz, H.; Seidel-Morgenstern, A.; Leschinsky, M.; Unkelbach, G. Method for Precipitating Lignin from Organosolv Pulping Liquors. Patent WO2016062676A1, 2014.
- (30) Schulze, P.; Seidel-Morgenstern, A.; Lorenz, H.; Leschinsky, M.; Unkelbach, G. Advanced Process for Precipitation of Lignin from Ethanol Organosolv Spent Liquors. *Bioresour. Technol.* **2016**, *199*, 128–34.
- (31) Schulze, P. Lignin Separation from Ethanol Water Pulping Liquors. Ph.D. Dissertation, Otto-von-Guericke Universität, Magdeburg, 2018.
- (32) Baumberger, S.; Abaecherli, A.; Fasching, M.; Gellerstedt, G.; Gosselink, R.; Hortling, B.; Li, J.; Saake, B.; de Jong, E. Molar Mass Determination of Lignins by Size-Exclusion Chromatography: Towards Standardisation of the Method. *Holzforschung* **2007**, *61* (4), 459–468.

- (33) Constant, S.; Wienk, H. L. J.; Frissen, A. E.; Peinder, P. d.; Boelens, R.; van Es, D. S.; Grisel, R. J. H.; Weckhuysen, B. M.; Huijgen, W. J. J.; Gosselink, R. J. A.; Bruijninx, P. C. A. New Insights into the Structure and Composition of Technical Lignins: A Comparative Characterisation Study. *Green Chem.* **2016**, *18* (9), 2651–2665.
- (34) Russel, W. B.; Saville, D. A.; Schowalter, W. R. *Colloidal Dispersions*; Cambridge University Press: New York, 1989.
- (35) Junker, E. Zur Kenntnis Der Kolloidchemischen Eigenschaften Des Humus. *Colloid Polym. Sci.* **1941**, *95* (2), 213–250.
- (36) Wang, G.; Chen, H. Fractionation of Alkali-Extracted Lignin from Steam-Exploded Stalk by Gradient Acid Precipitation. *Sep. Purif. Technol.* **2013**, *105*, 98–105.
- (37) Beisl, S.; Miltner, A.; Friedl, A. Lignin from Micro- to Nanosize: Production Methods. *Int. J. Mol. Sci.* **2017**, *18* (6), 1244.
- (38) Zdravkov, A. N. Interfacial Phenomena During Drop Coalescence in Polymeric Systems. Doctoral thesis, Technische Universiteit Eindhoven, 2004.
- (39) Hatakeyama, T.; Nakamura, K.; Hatakeyama, H. Studies on Heat Capacity of Cellulose and Lignin by Differential Scanning Calorimetry. *Polymer* **1982**, *23* (12), 1801–1804.
- (40) Gruber, E. *Polymerchemie*; Steinkopff: Darmstadt, 1980.
- (41) Verein\_Deutscher\_Ingenieure\_(VDI) *Vdi-Richtlinie: Vdi 2762 Blatt 2 Filtrierbarkeit Von Suspensionen - Bestimmung Des Filterkuchenwiderstands*, 2010.
- (42) Beckmann, W. *Crystallization: Basic Concepts and Industrial Applications*; Wiley: Weinheim, 2013.
- (43) Smit, A.; Huijgen, W. Effective Fractionation of Lignocellulose in Herbaceous Biomass and Hardwood Using a Mild Acetone Organosolv Process. *Green Chem.* **2017**, *19* (22), 5505–5514.